



# Two Percolation Behaviors in Binary Heterogeneous Composites for High Permittivity and Negative Permittivity

Xinshuai Li,<sup>1</sup> Shuwei Meng,<sup>2</sup> Peitao Xie,<sup>2,3,\*</sup> Yulei Wei,<sup>4</sup> Wenfeng Xu,<sup>1</sup> Guixian Li,<sup>5</sup> Gemeng Liang,<sup>6</sup> Ai Du,<sup>7,\*</sup> Kai Sun,<sup>8</sup> Zhicheng Shi<sup>1,\*</sup> and Runhua Fan<sup>8</sup>

## Abstract

Percolative composite is usually studied to achieve high permittivity when the fraction of fillers reaches the percolation threshold; besides, negative permittivity has also been a research hotspot and can be obtained above the percolation threshold. However, no studies have clarified whether the two percolation behaviors are the same one. Herein, the binary heterogeneous composites consisting of titanium nitride (TiN) particles and epoxy were prepared by compression molding, dielectric performance and percolation behavior were studied. Two percolation behaviors were demonstrated with increasing the TiN content. The first percolation behavior is to describe the high permittivity while the second one is to describe negative permittivity. It is interesting to find that the two percolation behaviors are actually associated with the competitive effect between inductance and capacitance. As a consequence, a high permittivity of 419 and a negative permittivity of -18 are obtained near the two percolation thresholds (42% and 50%), respectively. This work presents a clear physical description for the percolation phenomenon in the view of dielectric performance.

**Keywords:** Negative permittivity; Percolation theory; Dielectric constant; Metacomposites.

Received: 07 July 2022; Revised: 19 November 2022; Accepted: 29 November 2022.

Article type: Research article.

## 1. Introduction

Composite are usually produced from at least two constituent materials with notably different functional properties, such as electrical or mechanical properties, wherein one typical material is chosen as a matrix and a material is chosen as filler, combining the unique properties of both components. The percolation phenomenon, a classic and significant behavior in physics, is widely used to evaluate the physical performance in heterogeneous composites.<sup>[1-5]</sup> When the functional fillers

come into contact with each other with increasing filler content and establish a continuous cluster or network throughout the composite, there will be an abrupt shift in the physical properties of the composites and it is possible to achieve some magical performances, such as high permittivity, high electrical or thermal conductivity and negative permittivity.<sup>[6,7]</sup> This special volume fraction of fillers is called percolation threshold  $f_c$ , which is of great significance for percolative composites. For example, the study of percolation behavior can to some extent meet the increasing demand for high performance, such as high electrical or thermal conductivity or high permittivity. Due to the above characteristics, percolation composites have been widely used in many fields.<sup>[8-11]</sup>

As well known, percolative composite is usually studied to adjust the dielectric property. Dielectric constant is the constitutive electrical parameter for dielectric medium, usually positive.<sup>[12]</sup> When the fraction of fillers reaches the percolation threshold, the high permittivity can be achieved in these composites.<sup>[13,14]</sup> For instance, Grannan et al. observed that samples consisting of small Ag particles randomly

<sup>1</sup> School of Materials Science and Engineering, Ocean University of China, Qingdao 266100, P. R. China.

<sup>2</sup> State Key Laboratory of Bio-fibers and Eco-textiles Institute of Biochemical Engineering, Institute of Biochemical Engineering, College of Materials Science and Engineering, Qingdao University, Qingdao 266071, P. R. China.

<sup>3</sup> Foshan (Southern China) Institute for New Materials, Foshan, 528200, P. R. China.

<sup>4</sup> Shandong Sinocera Functional Material Co., LTD., Dongying, 257100, P. R. China.

<sup>5</sup> The 8511 research Institute of China Aerospace Science and Industry Corporation Limited (CASIC), Nanjing, 210007, P. R. China.

embedded in a nonconducting KCl matrix have a much higher dielectric constant than pure KCl (about 10 times higher).<sup>[15]</sup> Dang and coworkers constructed a class of multiwalled-carbon nanotubes/poly(vinylidene fluoride) (PVDF) composites, enabling a markedly enhancement of permittivity (more than 8000 at 100 Hz) compared to PVDF (10 at 100 Hz) by adjusting the volume fraction of conductive phase to near the percolation threshold (about 8%). The giant permittivity is mainly attributed to the significant blocking of charge carries at internal interfaces.<sup>[14]</sup>

In fact, dielectric constant can also be negative, which is first achieved in metamaterials.<sup>[16]</sup> Recently, negativity permittivity materials have become an attractive research point owing to their broad potential applications in wave absorbing, negative capacitance field-effect transistors. Negative permittivity is actually the instinctive property of some semiconductors and metals below their plasma frequency.<sup>[17-19]</sup> Negative permittivity behavior comes from the oscillation of free electrons in conductors, where free electrons do simple harmonic motion, making the direction of polarization electric field same to the external electrical field.<sup>[20,21]</sup> Moreover, it is further found that negative permittivity can also be realized by the inherent characteristics of the component materials in traditional percolative composites, where dielectric constant transfers from positive value to negative value with increasing filler content near percolation threshold.<sup>[22-26]</sup> For example, Xie *et al.* reported a Fe/coated-Fe/epoxy ternary composites in which the volume fraction of Fe/coated-Fe was kept constant (70%). when content of Fe particles was beyond the percolation threshold (about 75% of Fe/coated-Fe), the permittivity undergoes a sudden change from positive to negative (about 500 to -100).<sup>[27]</sup>

Therefore, there is a scientific question emerged whether the two percolation thresholds for high permittivity and negative permittivity are the same one. However, no studies have been made to solve this question. As for high permittivity in percolative composites, studies only revealed the fact that high permittivity can be realized near percolation threshold, but the negative permittivity has not been reported in these studies.<sup>[13,14]</sup> As for negative permittivity in percolative

composites, studies proved that negative permittivity can be achieved when the content of conductive fillers is above the percolation threshold, but no attention has been paid on studying the differences of percolation threshold for high permittivity and negative permittivity.<sup>[28-31]</sup> Therefore, this scientific question has not been solved.

In this work, the percolation behaviors were systematically studied in TiN/Epoxy composites to differentiate the high permittivity and negative permittivity. It is found that the percolation thresholds for high permittivity and negative permittivity are not the same. That is, there were two percolation behaviors for binary composites in the view of variation of dielectric constant with increasing the filler content. The dielectric constant firstly increased with increasing filler content and thus high permittivity could be achieved near the first percolation threshold, further increasing the filler content made the dielectric constant decrease but still kept positive, gradually the dielectric constant turned negative when the filler content was above second percolation threshold.

## 2. Experimental methods

Titanium nitride (TiN) powder are purchased from Aladdin Industrial Corporation (99.5%, 2-10  $\mu\text{m}$ , Shanghai, CHN). Bisphenol A type solid epoxy resin is purchased from Shanghai Yoo-Pont Chemical Industry Co., LTO (Shanghai, CHN) and used because of its good electric insulativity, chemical stability and easy processing. TiN is chosen as it is a conductive ceramic, excluding the influence of oxide layers that commonly happen in metal particle.<sup>[30,31]</sup> TiN powder is uniformly mixed with epoxy powder by ball-milling and the mixed powder is processed into bulk composites by compression molding and the samples dimension is  $\phi$  20 mm  $\times$  1.5 mm. Symmetrical round gold electrodes (diameter of 10.6mm) were sputtered on the two sides of composites for electrical measurements. For example, the sample "0.2" indicated that the volume fraction of TiN particles was 20%. The microstructure is observed by scanning electron microscopy (S-4800, Hitachi, Ltd.). The dielectric properties at the frequency range from 100 Hz to 1 MHz are tested by Agilent E4980A Precision LCR analyzer.<sup>[29]</sup>

## 3. Result and discussion

### 3.1 Electrical conductivity

Figure 1(a) shows the frequency dependence of ac conductivity ( $\sigma_{ac}$ ) for TiN/Epoxy composites with different TiN contents. The  $\sigma_{ac}$  increases with frequency for the composites with a content of not more than 0.43, while the  $\sigma_{ac}$  remains stable as the frequency increases for composites with

<sup>6</sup> School of Chemical Engineering & Advanced Materials, The University of Adelaide, Adelaide, Australia.

<sup>7</sup> Shanghai Key Laboratory of Special Artificial Microstructure Materials and Technology, School of Physics Science and Engineering, Tongji University, Shanghai 200092, China.

<sup>8</sup> College of Ocean Science and Engineering, Shanghai Maritime University, Shanghai.

\*E-mail: xiepeitao1991@qdu.edu.cn (P. Xie); duai@tongji.edu.cn (A. Du); zcshi@ouc.edu.cn (Z. Shi)

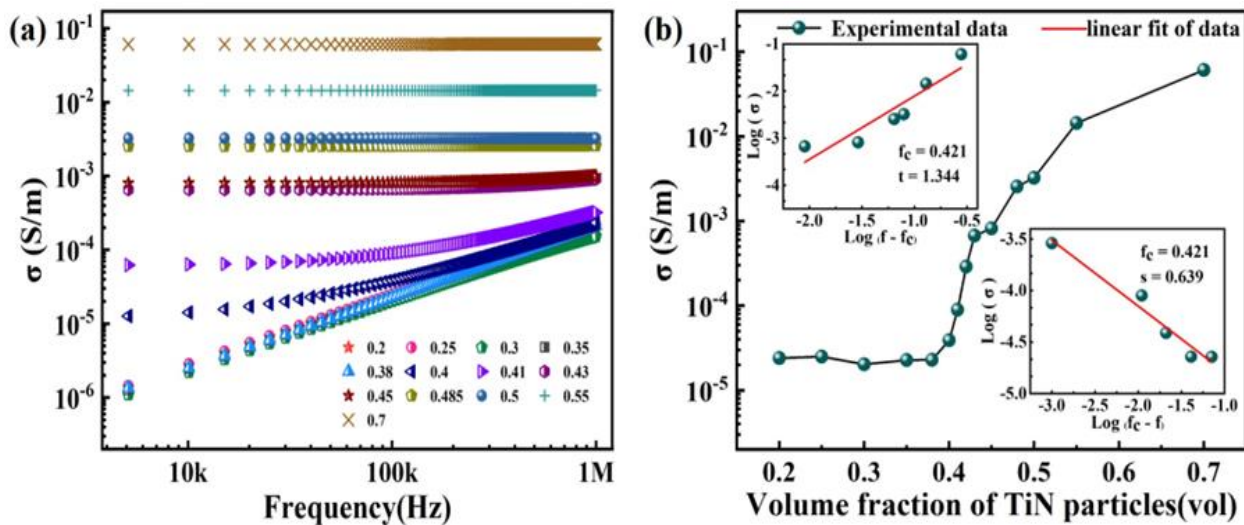


**Fig. 1** (a) The frequency dispersion of ac conductivity  $\sigma_{ac}$ , (b) the variation of  $\sigma_{ac}$  (at 10 kHz) for TiN/Epoxy composites with different contents of TiN. The insets in (b) indicates that the experimental data agree well with percolation theory.

a higher TiN content. The different frequency dispersions suggest different conductivity mechanisms and a percolating phenomenon.<sup>[28]</sup> Fig. 1(b) shows the variation of  $\sigma_{ac}$  at 100 kHz with TiN content, it can be clearly seen that the  $\sigma_{ac}$  is almost constant when TiN volume fraction  $f < 0.4$  but shows a dramatic increase of nearly two orders of magnitude when TiN content increases from 0.4 to 0.44. Likewise, this represents the occurrence of percolation. The equation (1) shows the relationship between electrical conductivity of percolative composite between content of fillers. In order to estimate the percolation threshold  $f_c$ , we fitted the experimental conductivity data to the Equations (1a) and (1b):<sup>[3,13,14]</sup>

$$\sigma_{ac} \propto (f_{c1} - f)^{-s} \tag{1a}$$

$$\sigma_{ac} \propto (f - f_{c1})^t \tag{1b}$$

where  $f$  is the volume fraction of TiN filler,  $f_{c1}$  is the percolation threshold,  $t$  is the critical exponent in the conducting region,  $s$  is the critical exponent in the insulating region. The calculation results (see the inset in Fig. 1(b),  $f_{c1} = 0.421$ ,  $t = 0.344$ ,  $s = 0.639$ ) using Equation (1) reveal good agreement with the experimental data, suggesting that percolation theory is applicable to the TiN/Epoxy composites, that is, there is percolation behavior in the TiN/Epoxy composites. In fact, the percolation threshold is influenced by the intrinsic properties of fillers and matrix, such as shape, size, surface state and dimension. For instance, when the filler size becomes smaller or changes from a spherical shape to an ellipsoidal shape, the percolation threshold is decreased. Due to the bigger size and spherical morphology of TiN, the percolation threshold of the composite is relatively high.<sup>[3]</sup>

### 3.2 Dielectric permittivity

Figures 2(a) and 2(b) depicts the real permittivity of

TiN/Epoxy composites as function of frequency. The dielectric curves are obviously different with the change of TiN content. For the composites with low TiN loadings (as shown Fig. 2(a),  $f < 0.43$ ), real permittivity is positive and its value increases with increasing TiN content due to the enhanced interfacial polarization.<sup>[32]</sup> The polarization across the interface between TiN particle and epoxy indicates that any pairs of adjacent TiN particles separated by an insulating gap can work as a microcapacitor. The composites can be regarded as a network of microcapacitors, which makes the dielectric permittivity of composites is higher with the increase of TiN content, a common phenomenon also known as Maxwell-Wagner-Sillars effect.<sup>[13,14]</sup> Meanwhile, it can be seen that the  $\epsilon'$  shows obvious frequency dispersion when the TiN content increases to 0.4, the  $\epsilon'$  decreases with increasing frequency. It is observed from Fig. 2(b) that further increasing the TiN loading resulted in negative permittivity with volume fraction of TiN filler ( $f$ ) = 0.5, 0.55 and 0.7, which is attributed to the low-frequency plasma oscillation of free electrons in continuous conductive pathway. With increasing of TiN contents, the absolute values of negative permittivity increased. The negative permittivity behavior in percolating composites can be expressed by the Drude model, which has been shown in previous studies.<sup>[23-25,27]</sup> It is worth noting that the real permittivity value does not suddenly become negative, there is an abrupt decrease for positive dielectric constant when the TiN content increases from 0.43 to 0.485, this interesting variation is studied in detail in the following text.

The dielectric permittivity as a function of the TiN content at 100 kHz is showed in Fig. 2(c). As we analyzed earlier, the real permittivity goes up first, then goes down but still remains positive, and finally becomes negative with increasing TiN

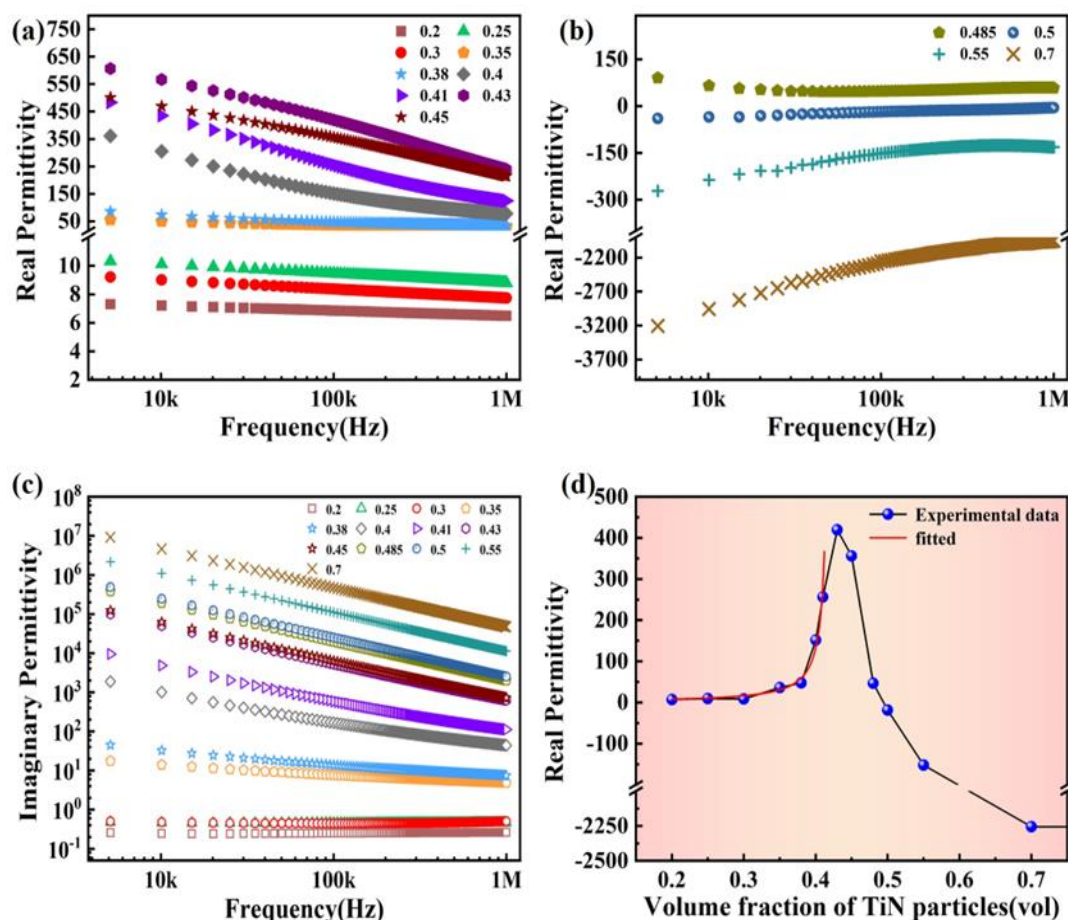


**Fig. 2** Frequency dependence of the real parts (a, b) and imaginary part (c) of dielectric permittivity for the TiN/Epoxy composites. (d) The variation of real permittivity with different TiN contents at 10 kHz. The red solid line in (d) is fitted by Equation (3), indicating a typical percolation behavior.

content. The enhanced positive permittivity with increasing filler content in binary heterogeneous composite can be described by the percolation theory, the Equation (2) shows the relationship between dielectric constant of percolative composite between content of fillers.<sup>[14,24]</sup>

$$\epsilon \propto (f_{c2} - f)^{-q} \quad (2)$$

where  $f$  is the volume fraction of TiN filler,  $f_{c2}$  is the percolation threshold for enhanced dielectric permittivity,  $q$  is the critical exponent. It can be concluded from the formula that high positive permittivity can be achieved near but still below the percolation threshold. The fitting parameters  $f_{c2}$  is 0.421, indicating the percolation threshold for high permittivity is 0.421, named the first percolation threshold for dielectric binary composites consisting of conductive fillers and insulative matrix. The  $f_{c2}$  is equal to the  $f_{c1}$  of describing the percolation for electrical conductivity that appeared before, which demonstrates that the percolations for high permittivity and enhanced electrical conductivity happen at the same time. This percolation is mainly attributed to the change of microstructure in the composites, which is shown in Fig. S1. The TiN particles are isolated to each other when the TiN content is low, while agglomeration and network can be formed when the TiN content is high. Therefore, the electrical conductivity will increase and the interfacial polarization

functions as microcapacitors to enhance the positive dielectric permittivity. Further increasing the TiN content, a few connected TiN particles will form the conductive pathways, as a result, some microcapacitors are converted to inductances and no longer contribute to positive dielectric permittivity, the dielectric permittivity goes down but still remains positive value. When the TiN content further increases to a higher level of 0.5 and above, more conductive pathways are formed and the inductive contributions are dominative, the negative permittivity is achieved as inductance has close relationship with negative permittivity.<sup>[33,34]</sup> Therefore, the close-range isolated dispersion of the fillers produces a high-permittivity, and enough conductive paths are formed to generate a negative permittivity. The critical volume fraction of conductive filler to achieve negative permittivity is named as the second percolation threshold. It can be concluded that there are two percolation behaviors in the binary heterogeneous composites in the view of the change of dielectric performance and the percolation thresholds for high permittivity and negative permittivity are not the same one.

The frequency dispersion of imaginary permittivity and dielectric loss tangent ( $\tan \delta$ ) are shown in Fig. 2(d) and Fig. S2. The  $\epsilon''$  descends with increasing frequency. With regard to a percolating composites system, the dielectric loss mainly

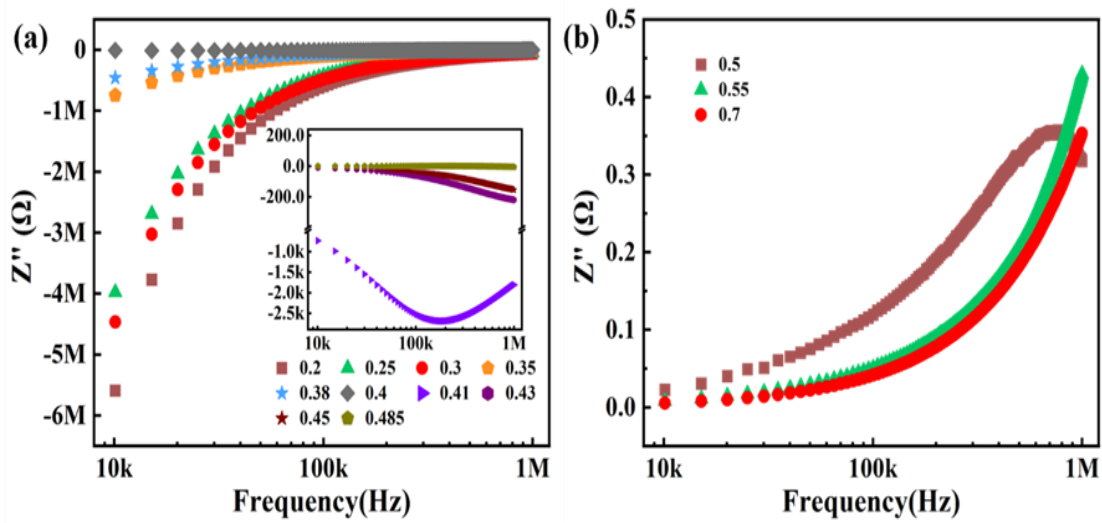


**Fig. 3** (a, b) Frequency dependence of reactance for the TiN/Epoxy composites with different TiN content. The inset in (a) is a partial enlargement.

includes the polarization loss and conduction loss.<sup>[35]</sup> For samples with low TiN content,  $\epsilon''$  remains stable as the frequency increases. The reason could be that the contribution from the polarization loss becomes more evident at the high frequency, while the conduction loss decreases as the frequency increases. As for the  $\tan \delta$ , the  $\tan \delta$  value shows obvious enhancement with increasing the TiN content. The conduction loss plays a dominant role in the dielectric loss with the increase of TiN content, as the electrical conductivity of the composites enhanced.

**3.3 Impedance and equivalent circuit analysis**

Figure 3 and Figure S3 shows the frequency dependence of reactance ( $Z''$ ) and modulus of impedance ( $|Z|$ ) for the composites with different TiN contents. There is a clear shift for  $Z''$  from negative to positive with increasing the TiN content, the  $Z''$  is negative for low TiN content while turns to positive for high content of 0.5 and above. Materials which are

placed into an external electric field can be regarded as a circuit consisting of capacitors, resistors and inductors.<sup>[27-29]</sup> In the circuit, the inductor and capacitor will oppose the change of electric field, which is known as inductive reactance ( $Z_L$ ) and capacitive reactance ( $Z_C$ ). The reactance is expressed as  $Z'' = Z_L - Z_C$ .<sup>[30]</sup> As  $Z'' < 0$  and  $f \leq 0.485$ , the capacitive reactance is large than inductive reactance, indicating capacitive character and a lag of the voltage behind that of the current, the composites with positive permittivity can be regarded as a capacitor with leakage current, manifesting a capacitive behavior.<sup>[36,37]</sup> Correspondingly, when  $Z'' > 0$  and  $f \geq 0.5$ , the composites with negative permittivity manifest an inductive behavior.

In order to further analyze the impedance properties of composites, the equivalent circuit analysis was performed to investigate the impedance spectra using the ZSimpwin software. As shown in Fig. 4(a), the composites with TiN content less than 0.485 were equivalent to circuit model

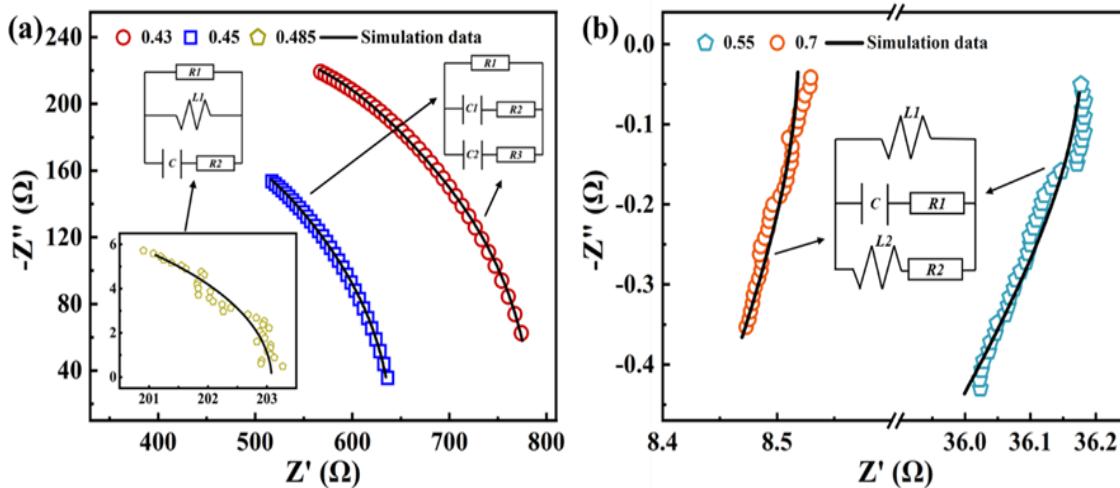


**Fig. 4** (a, b) Nyquist plots for the composites and equivalent circuit analysis. The inset shows equivalent circuits for composites with different volume fraction, and the solid lines are simulation results using the equivalent circuit.

consisting of resistor R and capacitor C, the R came from the leakage current of composites and C mainly resulted from the microcapacitors formed by TiN particles in the composites. When  $f = 0.485$ , the inductor started to be introduced in equivalent circuit, as shown in the inset of Fig. 4(a), which represent the existence of conductive path. But in fact, the reactance still remained negative, indicating the inductive character caused by the conductive path was weaker than the capacitive character resulted from the microcapacitors. The generation of inductance is also the reason for the decrease in the dielectric constant mentioned above. It was observed from Fig. 4(b) that the reactance was positive when  $f \geq 0.5$ , manifesting that the composites were inductive. The number of inductors increased compared with  $f = 0.485$ , suggesting that the conductive path increases with the increase of the conductive particles, which was further demonstrated by the SEM results in Fig. S1. Therefore, the inductive conductive network is the decisive building block to achieve negative permittivity, there is a competitive effect for reactance in the percolative dielectric composites consisting of conductive fillers, only the negative permittivity behavior occurs when the inductive character is stronger than the capacitive character, which is the main reason for the two percolation behaviors for the variation of dielectric permittivity.<sup>[38,39]</sup>

#### 4. Conclusion

In summary, this study reports two percolation behaviors in binary heterogeneous composites consisting of conductive filler and insulative matrix with increasing the filler content. The first percolation behavior is to describe the high permittivity while the second one is to describe negative permittivity. The dielectric constant firstly increased with increasing filler content and thus high permittivity was achieved near the first percolation threshold, further increasing the filler content made the dielectric constant decrease but still kept positive, gradually the dielectric constant turned negative when the filler content was above the second percolation threshold. The equivalent circuit analysis demonstrated that the competitive effect between inductance and capacitance is the main reason for the two percolation behaviors. Consequently, a high permittivity of 419 and a negative permittivity of -18 are obtain near two percolation thresholds. This work provides a clear physical exposition for the percolation theory in the view of dielectric performance.

#### Acknowledgments

This work was supported by the National Natural Science Foundation of China (51773187, 51871146, 52101176), the China Postdoctoral Science Foundation (2020M671992),

Postdoctoral Innovation Project of Shandong Province (202003031), Natural Science Foundation of Shandong Province (ZR2020QE006), Guangdong Basic and Applied Basic Research Foundation (2021A1515110883), the Fundamental Research Funds for the Central Universities (201961060), Innovation Program of the Shanghai Municipal Education Commission (Grant No. 18CG56), the Opening Project of Shanghai Key Laboratory of Special Artificial Microstructure Materials and Technology.

#### Conflict of Interest

There is no conflict of interest.

#### Supporting Information

Applicable, available at

#### References

- [1] R. Bhat, N. Mohan, S. Sharma, S. Rao, Influence of seawater absorption on the hardness of glass fiber/polyester composite, *Journal of Computers, Mechanical and Management*, 2022, **1**, 1-11, doi: 10.57159/gadl.jcmm.1.1.22003.
- [2] V. Srikanth, S. Kowshik, D. Narasimha, S. Patil, K. Samanth, U. Rathee, Finite element modelling and analysis of fiber reinforced concrete under tensile and flexural loading, *Journal of Computers, Mechanical and Management*, 2022, 12-18, doi: 10.57159/gadl.jcmm.4.1.22004.
- [3] C.-W. Nan, Y. Shen, J. Ma, Physical properties of composites near percolation, *Annual Review of Materials Research*, 2010, **40**, 131-151, doi: 10.1146/annurev-matsci-070909-104529.
- [4] H. Du, X. Lin, H. Zheng, B. Qu, Y. Huang, D. Chu, Colossal permittivity in percolative ceramic/metal dielectric composites, *Journal of Alloys and Compounds*, 2016, **663**, 848-861, doi: 10.1016/j.jallcom.2015.12.171.
- [5] L. Liu, J. Qu, A. Gu, B. Wang, Two-dimensional nanosheets of bimetallic chalcogenide-tagged nitrogen-doped carbon as a cathode for high-performance and durable zinc-ion capacitors, *Journal of Materials Chemistry A*, 2020, **8**, 18515.
- [6] Z.-C. Shi, F. Mao, J. Wang, R.-H. Fan, X. Wang, Percolative silver/alumina composites with radio frequency dielectric resonance-induced negative permittivity, *RSC Advances*, 2015, **5**, 107307-107312, doi: 10.1039/c5ra21808j.
- [7] Y. Shen, Y. H. Lin, C.-W. Nan, Interfacial effect on dielectric properties of polymer nanocomposites filled with core/shell-structured particles, *Advanced Functional Materials*, 2007, **17**, 2405-2410, doi: 10.1002/adfm.200700200.
- [8] P. Xie, Y. Liu, M. Feng, M. Niu, C. Liu, N. Wu, K. Sui, R. R. Patil, D. Pan, Z. Guo, R. Fan, Hierarchically porous Co/C nanocomposites for ultralight high-performance microwave absorption, *Advanced Composites and Hybrid Materials*, 2021, **4**, 173-185, doi: 10.1007/s42114-020-00202-z.
- [9] N. Wu, B. Zhao, J. Liu, Y. Li, Y. Chen, L. Chen, M. Wang, Z. Guo, MOF-derived porous hollow Ni/C composites with optimized impedance matching as lightweight microwave

- absorption materials, *Advanced Composites and Hybrid Materials*, 2021, **4**, 707-715, doi: 10.1007/s42114-021-00307-z.
- [10] G. Qi, Y. Liu, L. Chen, P. Xie, D. Pan, Z. Shi, B. Quan, Y. Zhong, C. Liu, R. Fan, Z. Guo, Lightweight Fe<sub>3</sub>C@Fe/C nanocomposites derived from wasted cornstalks with high-efficiency microwave absorption and ultrathin thickness, *Advanced Composites and Hybrid Materials*, 2021, **4**, 1226-1238, doi: 10.1007/s42114-021-00368-0.
- [11] Y. Huang, M. Chen, A. Xie, Y. Wang, X. Xu, Recent advances in design and fabrication of nanocomposites for electromagnetic wave shielding and absorbing, *Materials*, 2021, **14**, 4148, doi: 10.3390/ma14154148.
- [12] G. Raju, Dielectrics in electric fields: Tables, Atoms, and Molecules, second ed., CRC press, 2017.
- [13] Z.-M. Dang, Y.-H. Lin, C.-W. Nan, Novel ferroelectric polymer composites with high dielectric constants, *Advanced Materials*, 2003, **15**, 1625-1629, doi: 10.1002/adma.200304911.
- [14] Z.-M. Dang, L. Wang, Y. Yin, Q. Zhang, Q.-Q. Lei, Giant dielectric permittivities in functionalized carbon-nanotube/electroactive-polymer nanocomposites, *Advanced Materials*, 2007, **19**, 852-857, doi: 10.1002/adma.200600703.
- [15] D. M. Grannan, J. C. Garland, D. B. Tanner, Critical behavior of the dielectric constant of a random composite near the percolation threshold, *Physical Review Letters*, 1981, **46**, 375-378, doi: 10.1103/physrevlett.46.375.
- [16] H. Wu, Y. Zhong, Y. Tang, Y. Huang, G. Liu, W. Sun, P. Xie, D. Pan, C. Liu, Z. Guo, Precise regulation of weakly negative permittivity in CaCu<sub>3</sub>Ti<sub>4</sub>O<sub>12</sub> metacomposites by synergistic effects of carbon nanotubes and grapheme, *Advanced Composites and Hybrid Materials*, 2022, **5**, 419-430, doi: 10.1007/s42114-021-00378-y.
- [17] Z.-C. Shi, R.-H. Fan, K.-L. Yan, K. Sun, M. Zhang, C.-G. Wang, X.-F. Liu, X.-H. Zhang, Preparation of iron networks hosted in porous alumina with tunable negative permittivity and permeability, *Advanced Functional Materials*, 2013, **23**, 4123-4132, doi: 10.1002/adfm.201202895.
- [18] Y. Qu, J. Wu, Z. Wang, Y. Liu, P. Xie, Z. Wang, J. Tian, R. Fan, Radio-frequency epsilon-negative property and diamagnetic response of percolative Ag/CCTO metacomposites, *Scripta Materialia*, 2021, **203**, 114067, doi: 10.1016/j.scriptamat.2021.114067.
- [19] Y. Qu, Z. Wang, P. Xie, Z. Wang, R. Fan, Ultraweakly and fine-tunable negative permittivity of polyaniline/nickel metacomposites with high-frequency diamagnetic response, *Composites Science and Technology*, 2022, **217**, 109092, doi: 10.1016/j.compscitech.2021.109092.
- [20] J. B. Pendry, A. J. Holden, W. J. Stewart, I. Youngs, Extremely low frequency plasmons in metallic mesostructures, *Physical Review Letters*, 1996, **76**, 4773-4776, doi: 10.1103/physrevlett.76.4773.
- [21] J. Pendry, Low frequency plasmons in thin-wire structures: a commentary, *Journal of Physics: Condensed Matter*, 2016, **28**, 481002.
- [22] P. Xie, W. Sun, A. Du, Q. Hou, G. Wu, R. Fan, Epsilon-negative carbon aerogels with state transition from dielectric to degenerate semiconductor, *Advanced Electronic Materials*, 2021, **7**, 2000877, doi: 10.1002/aelm.202000877.
- [23] P. Xie, Y. Li, Q. Hou, K. Sui, C. Liu, X. Fu, J. Zhang, V. Murugadoss, J. Fan, Y. Wang, R. Fan, Z. Guo, Tunneling-induced negative permittivity in Ni/MnO nanocomposites by a bio-gel derived strategy, *Journal of Materials Chemistry C*, 2020, **8**, 3029-3039, doi: 10.1039/c9tc06378a.
- [24] Z. Wang, K. Sun, P. Xie, Y. Liu, Q. Gu, R. Fan, Permittivity transition from positive to negative in acrylic polyurethane-aluminum composites, *Composites Science and Technology*, 2020, **188**, 107969, doi: 10.1016/j.compscitech.2019.107969.
- [25] G. Fan, Z. Wang, K. Sun, Y. Liu, R. Fan, Doped ceramics of indium oxides for negative permittivity materials in MHz-kHz frequency regions, *Journal of Materials Science & Technology*, 2021, **61**, 125-131, doi: 10.1016/j.jmst.2020.06.013.
- [26] K. Sun, R. Fan, Y. Yin, J. Guo, X. Li, Y. Lei, L. An, C. Cheng, Z. Guo, Tunable negative permittivity with fano-like resonance and magnetic property in percolative silver/yttrium iron garnet nanocomposites, *The Journal of Physical Chemistry C*, 2017, **121**, 7564-7571, doi: 10.1021/acs.jpcc.7b02036.
- [27] P. Xie, Z. Wang, K. Sun, C. Cheng, Y. Liu, R. Fan, Regulation mechanism of negative permittivity in percolating composites via building blocks, *Applied Physics Letters*, 2017, **111**, 112903, doi: 10.1063/1.4994234.
- [28] P. Xie, Z. Wang, Z. Zhang, R. Fan, C. Cheng, H. Liu, Y. Liu, T. Li, C. Yan, N. Wang, Z. Guo, Silica microsphere templated self-assembly of a three-dimensional carbon network with stable radio-frequency negative permittivity and low dielectric loss, *Journal of Materials Chemistry C*, 2018, **6**, 5239-5249, doi: 10.1039/c7tc05911f.
- [29] P. Xie, K. Sun, Z. Wang, Y. Liu, R. Fan, Z. Zhang, G. Schumacher, Negative permittivity adjusted by SiO<sub>2</sub>-coated metallic particles in percolative composites, *Journal of Alloys and Compounds*, 2017, **725**, 1259-1263, doi: 10.1016/j.jallcom.2017.04.248.
- [30] C. Cheng, K. Yan, R. Fan, L. Qian, Z. Zhang, K. Sun, M. Chen, Negative permittivity behavior in the carbon/silicon nitride composites prepared by impregnation-carbonization approach, *Carbon*, 2016, **96**, 678-684, doi: 10.1016/j.carbon.2015.10.003.
- [31] C. Cheng, R. Fan, Y. Ren, T. Ding, L. Qian, J. Guo, X. Li, L. An, Y. Lei, Y. Yin, Z. Guo, Radio frequency negative permittivity in random carbon nanotubes/alumina nanocomposites, *Nanoscale*, 2017, **9**, 5779-5787, doi: 10.1039/c7nr01516j.
- [32] J. Guo, H. Song, H. Liu, C. Luo, Y. Ren, T. Ding, M. A. Khan, D. P. Young, X. Liu, X. Zhang, J. Kong, Z. Guo, Polypyrrole-interface-functionalized nano-magnetite epoxy nanocomposites as electromagnetic wave absorbers with enhanced flame retardancy, *Journal of Materials Chemistry C*, 2017, **5**, 5334-5344, doi: 10.1039/c7tc01502j.
- [33] H. Gu, H. Zhang, C. Ma, S. Lyu, F. Yao, C. Liang, X. Yang, J. Guo, Z. Guo, J. Gu, Polyaniline assisted uniform dispersion for magnetic ultrafine Barium ferrite nanorods reinforced epoxy metacomposites with tailorable negative permittivity, *The Journal of Physical Chemistry C*, 2017, **121**, 13265-13273, doi: 10.1021/acs.jpcc.7b03580.

- [34] P. Xie, Z. Shi, M. Feng, K. Sun, Y. Liu, K. Yan, C. Liu, T. A. A. Moussa, M. Huang, S. Meng, G. Liang, H. Hou, R. Fan, Z. Guo, Recent advances in radio-frequency negative dielectric metamaterials by designing heterogeneous composites, *Advanced Composites and Hybrid Materials*, 2022, **5**, 679-695, doi: 10.1007/s42114-022-00479-2.
- [35] Z. Zhang, M. Liu, M. M. Ibrahim, H. Wu, Y. Wu, Y. Li, G. A. M. Mersal, I. H. El Azab, S. M. El-Bahy, M. Huang, Y. Jiang, G. Liang, P. Xie, C. Liu, Flexible polystyrene/graphene composites with epsilon-near-zero properties, *Advanced Composites and Hybrid Materials*, 2022, **5**, 1054-1066, doi: 10.1007/s42114-022-00486-3.
- [36] L. Sun, Z. Shi, B. He, H. Wang, S. Liu, M. Huang, J. Shi, D. Dastan, H. Wang, Asymmetric trilayer all-polymer dielectric composites with simultaneous high efficiency and high energy density: a novel design targeting advanced energy storage capacitors, *Advanced Functional Materials*, 2021, **31**, 2100280, doi: 10.1002/adfm.202100280.
- [37] S. Sun, Z. Shi, L. Sun, L. Liang, D. Dastan, B. He, H. Wang, M. Huang, R. Fan, Achieving concurrent high energy density and efficiency in all-polymer layered paraelectric/ferroelectric composites via introducing a moderate layer, *ACS Applied Materials & Interfaces*, 2021, **13**, 27522-27532, doi: 10.1021/acsami.1c08063.
- [38] H. Wu, Z. Mu, G. Qi, Y. Zhang, X. Wang, P. Xie, N. Wu, H. Yuan, K. Sui, R. Fan, C. Liu, Negative permittivity behavior in Ti<sub>3</sub>AlC<sub>2</sub>-polyimide composites and the regulation mechanism, *Journal of Materials Science: Materials in Electronics*, 2021, **32**, 10388-10397, doi: 10.1007/s10854-021-05695-y.
- [39] M. Liu, X. Lan, H. Zhang, P. Xie, N. Wu, H. Yuan, K. Sui, R. Fan, C. Liu, Iron/epoxy random metamaterials with adjustable epsilon-near-zero and epsilon-negative property, *Journal of Materials Science: Materials in Electronics*, 2021, **32**, 15995-16007, doi: 10.1007/s10854-021-06150-8.

**Publisher's Note:** Engineered Science Publisher remains neutral with regard to jurisdictional claims in published maps and institutional affiliations.